Vietnam Journal of Science and Technology ***63*** *(3) (2025) 540-552*

doi:10.15625/2525-2518/19096

Application of composite based on magnetite oxide to remove the ofloxacin from aqueous solution

Bui Minh Quy[1, *], Tran Tuan Tu[2], Vu Thi Thu Le[3], Vu Quang Tung[1], Nguyen Thi Quynh Giang[4], Hoang Van Quang[1]

[1]*Thai Nguyen University of Sciences, Thai Nguyen University (TNU), Tan Thinh, Thai Nguyen, Viet Nam*

[2]*Thai Nguyen University of Medicine and Pharmacy, Thai Nguyen University (TNU), Luong Ngoc Quyen, Thai Nguyen, Viet Nam*

[3]*Thai Nguyen University of Agriculture and Forestry, Thai Nguyen University (TNU), Quyet Thang, Thai Nguyen, Viet Nam*

[4]*The National Institute of Drug Quality Control, Tam Hiep, Thanh Tri, Ha Noi, Viet Nam*

[*]Email*: quybm@tnus.edu.vn*

Received: 6 October 2023; Accepted for publication: 17 April 2024

Abstract. In this research, chitosan-Fe_3O_4 composite materials (CS-MNPs) were successfully synthesized using chemical processes. XRD, SEM, TEM, EDS and VSM techniques were employed to analyze the characteristics of the materials. To remove the antibiotic ofloxacin (OFX) from aqueous solutions, CS-MNPs were used as an adsorbent. The effects of pH, contact time, initial concentration, and the presence of another antibiotic (ciprofloxacin) in the solution were investigated to evaluate the ability of OFX to be adsorbed. The experimental data were analyzed using adsorption models, including kinetic models (pseudo-first-order, pseudo-second-order, and Elovich models), isotherm adsorption models (Langmuir, Freundlich, and Temkin models), and the Langmuir competitive adsorption model. After five adsorption-desorption cycles, the materials showed high reusability, with an OFX removal efficiency of 50.16 %.

Keywords: Chitosan, magnetite, antibiotic, ofloxacin, adsorption.

Classification numbers: 2.4.2, 2.4.4, 3.2.3

1. INTRODUCTION

Antibiotic contamination in water is an emerging issue that results in the further transmission of these micropollutants into the environment, thereby increasing the risk of spreading drug resistance and endangering public health [1]. Research on the repercussions of antibiotic pollution reveals a disconcerting prevalence of antibiotics detected in water samples worldwide [2]. The incidence of antibiotic resistance among the Vietnamese population has reached 40 % of the total, with Viet Nam ranking fourth in this rate within the Asia-Pacific region [3, 4]. Ofloxacin (OFX) is a quinolone antibiotic useful for the treatment of a number of

bacterial infections by selectively hindering the synthesis procedure of their DNA [5]. It is used as drugs for both humans and animals. Although antibiotics can be detected in water at low concentrations, they can accumulate and pose a risk to aquatic life and humans over time [6]. Thus, it is essential to remove antibiotics in general and OFX in particular from aqueous solutions.

The removal of antibiotic residues from aquatic environments has been investigated using a variety of techniques [7, 8]. Adsorption is a frequently employed technique for treating antibiotic pollution in water due to its simplicity of treatment process, convenience of usage, economic efficiency, and high removal capacity [9]. Many scientists have studied chitosan-based composite materials due to their excellent adsorption capacity, biocompatibility, and environmental friendliness. Chitosan has been combined with MgO, nano TiO_2, and graphene as adsorbents to remove antibiotics such as norfloxacin, levofloxacin, and ceftriaxone from water However, due to the low specific gravity of chitosan, after adsorption, it is recovered by centrifugation or filtration, resulting in a time-consuming process with low efficiency and high cost. To facilitate the recovery and reuse of adsorbent materials, chitosan can be combined with magnetic materials to create a magnetic composite. Common magnetic materials include Fe_3O_4 [10], γ-Fe_2O_3 [7], FeO [11], and cobalt ferrite [12]. Among these, the combination of chitosan and Fe_3O_4 is considered easy and simple with the resulting material being a highly magnetic material [13, 14]. This material has been utilized to treat pollutants such as heavy metals and organic pigments [10, 15]. However, there have not been many publications on its application for treating antibiotic residues in water. In Viet Nam, the synthesis and application of this substance as an adsorbent, especially for removing ofloxacin antibiotics from aqueous solutions, are relatively limited [16, 17].

This research marks a pioneering effort in the synthesis of chitosan-ferromagnetic oxide (CS-MNPs) materials designed for the removal of the antibiotic ofloxacin from aquatic environments. Comprehensive characterizations of the materials were conducted using XRD, SEM, TEM, EDS, and VSM methods. The study delved into various influencing factors affecting adsorption efficiency, including pH, adsorption duration, initial antibiotic concentration, and the presence of a second antibiotic in the aqueous solution. Furthermore, the collected data were fitted to isothermal adsorption models and adsorption kinetic models. The research also explored the potential reusability of CS-MNPs materials.

2. MATERIALS AND METHODS

2.1. Materials

All chemicals were of high purity and include: ofloxacin ($C_{18}H_{20}FN_3O_4$, 99.81 %, the National Institute of Drug Quality Control, Ha Noi, Viet Nam), $FeCl_2.4H_2O$ (99 %, China), $FeCl_3.6H_2O$ (99 %, China), NaOH (99 %, China), CH_3COOH (99 %, China), HCl (37 %, d = 1.19 g/mL, Merk, Germany), and chitosan (85 % DD, China).

2.2. Synthesis of adsorbent materials CS-MNPs

The materials were synthesized by the co-precipitation method combined with the in-situ method with a CS:MNPs mass ratio of 3:7. This synthesis procedure was applied according to our previous reports [16]. The reaction system included 40 mL of Fe^{2+} (0.25 M), 40 mL of Fe^{3+} (0.50 M), and 20 mL of chitosan solution (1.99 g of CS dissolved in 20 mL of 2 % acetic acid). Subsequently, 1 M NaOH solution was added to adjust the system's pH to 13. The formation of CS-MNPs was indicated by the appearance of a black precipitate in the solution. After a reaction

time of approximately 60 min, a magnet was employed to separate the synthesized material from the solution. The material underwent washing with distilled water until reaching a pH of 7 and was then dried at 70 °C for 24 hours.

2.3. Adsorption experiments

OFX solutions were prepared at various concentrations (C_0 = 5, 10, 15, 20, 30 mg/L) and different pH levels (pH = 1, 3, 5, 7, 8, 9, 11). In a flask, 0.02 g of CS-MNPs was mixed with 25 mL of the OFX solution. The OFX adsorption process was conducted for various time periods on a shaker (t = 5, 10, 20, 30, 40, 60, 90, 120, and 150 min) at 400 rpm. Subsequently, a magnetic field was employed to separate the post-adsorption solution.

Equations (1) and (2) were used to calculate the adsorption capacity (q, mg/g) and removal efficiency (RE, %) of antibiotics, respectively.

$$q = \frac{(C_o - C).V}{m} \quad (1)$$

$$RE = \frac{C_o - C}{C_o}.100\% \quad (2)$$

wherein: q represents the adsorption capacity (mg/g), C_0 and C denote the antibiotic concentrations before and after adsorption (mg/L), respectively, V stands for the solution volume (L), and m indicates the mass of the adsorbent (g).

Investigating the effect of the second antibiotic, ciprofloxacin (CFX), we maintained its initial concentration at 10 mg/L. Solutions were prepared with varying concentration ratios of the two antibiotics, OFX and CFX, namely OFX:CFX of 1.0:0.0, 0.5:1.0, 1.0:1.0, 1.5:1.0, 2.0:1.0, and 0.0:1.0, all at a pH of 7. Other adsorption parameters, such as CS-MNPs mass (m = 0.02 g), adsorption solution volume (V = 25 mL), and adsorption time (t = 90 min), were kept constant. Results from each experiment were averaged based on three replicates.

Regeneration study: Adsorption-regeneration investigations were conducted to investigate the reusability of CS-MNP adsorbents. The spent adsorbent was recycled by shaking with 25 mL of NH_3 solution (0.5 N) for 60 min, followed by magnetic separation, washing three times with deionized water, and drying for 24 hours at 70 °C. The regenerated adsorbent was applied to adsorb OFX under conditions identical to those for the original adsorbent. Cycles 1, 2, 3, 4, and 5 of this regeneration-adsorption experiment were carried out in succession. Final concentrations of antibiotic solutions were calculated following each adsorption and desorption cycle.

2.4. Instruments

Scanning electron microscopy (SEM, Hitachi S-4800, acceleration of 15 – 20 keV, working electrode distance of 4-5 mm) was used to characterize the surface morphology of CS-MNPs. This device is equipped with an energy dispersive X-ray spectroscopy (EDS) under an accelerating voltage of 10 kV to determine the elemental composition of the materials. X-ray diffraction (XRD, D2-Phase, Bruker, Karlsruhe, Germany, 2θ = 10 - 70^o) was used to analyze the crystalline structure of CS-MNPs. Transmission electron microscopy (TEM, JEOL 200CX, Japan, at 100 keV) was used to determine the shape and size of CS-MNPs. The vibrating sample magnetometer (VSM, Germany, at ± 10 kOe and 25 °C) was used to measure the magnetic properties of CS-MNPs. The UV-visible spectrometer (Jasco V-770, Japan) was used to

determine the concentrations of OFX and CFX before and after adsorption at a wavelength of 285 nm and 275 nm, respectively.

3. RESULTS AND DISCUSSION

3.1. Characterization of material

Positions 2-theta = {30.04°, 35.33 °, 43.08°, 53.37°, 57,16°, 62.62°} on the X-ray diffraction diagram of the synthesised CS-MNPs material (Figure 1, left) correspond to the lattice surfaces (hkl) = {(220), (311), (400), (422), (511), (440)}, which are assigned to the characteristic peak of the cubic spinel structure of Fe_3O_4 [18]. In the figure, in addition to the distinct peaks of Fe_3O_4, there is a broad peak of chitosan at 2-theta = 20.9° [19]. This demonstrates that the synthetic material does indeed exist as a composite of chitosan and iron oxide and the addition of chitosan has no effect on the crystal structure of Fe_3O_4. According to the results of SEM and TEM pictures (Figure 1, middle and right), the material's surface characteristics indicate the presence of spherical pores with a diameter of approximately 20 nm.

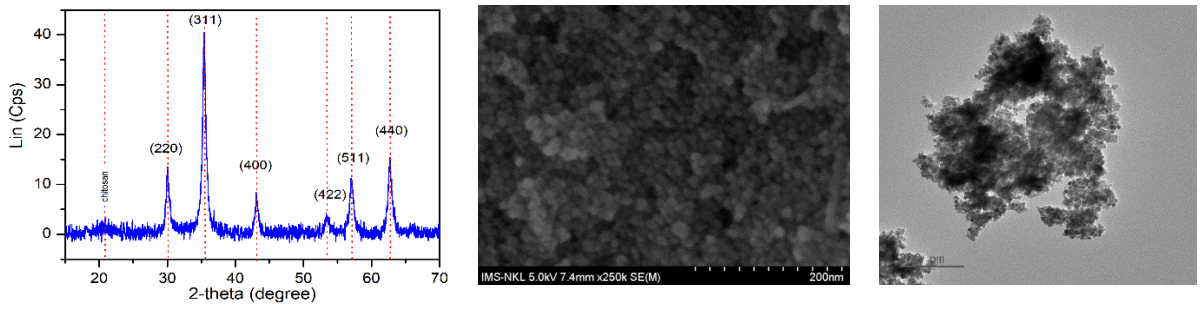

Figure 1. XRD pattern (left), SEM (middle), and TEM (right) of the material.

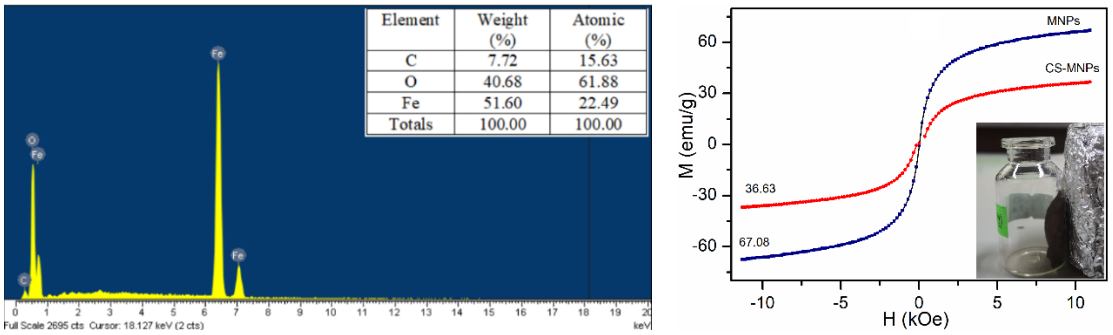

Figure 2. EDS (left) and VSM (right) results of CS-MNPs.

According to the EDS data (Figure 2, left), the synthesized substance consists of carbon (C), oxygen (O), and iron (Fe) with corresponding mass percentages of 7.72, 40.68, and 51.60 %, respectively. This results in a mass ratio of approximately 3:7 for CS to MNPs, consistent with the estimated mass ratio in Section 2.2. The ability of CS-MNPs to be recovered using a magnetic field depends on their magnetism. The VSM findings (Figure 2, right) show that CS-MNPs exhibit superparamagnetic properties with a magnetic saturation of 36.63 emu/g. While this value is lower than the magnetic saturation of MNPs alone (M = 67.08 emu/g), CS-MNPs still respond strongly to a magnetic field (the inset in Figure 2, right).

3.2. Adsorption of OFX from aqueous solution

3.2.1. Effect of pH

Figure 3 presents the results of the investigation into how pH affects the adsorption capacity of CS-MNPs for OFX. The findings indicate that OFX adsorption is ineffective, with efficiencies below 20 % and 50 % at acidic and alkaline pH levels, respectively. The maximum OFX adsorption efficiency of 60.68 % is achieved at neutral pH. This finding can be explained by the presence of OFX in solution (Figure 4) (pKa = 5.77 and 8.44 [20]) and the point of zero charge of CS-MNPs (pH_{pzc} = 6.5 [16]). At pH = 7, the zwitterionic form of $OFX^{\pm}$ and the negatively charged surface of CS-MNPs may interact electrostatically, enhancing adsorption efficiency. Adsorption efficiency decreases at pH values of 1, 3, 8, 9, and 11 due to repulsive interactions between substances with the same charge. Based on these findings, pH = 7 was selected as the optimal pH for further investigation.

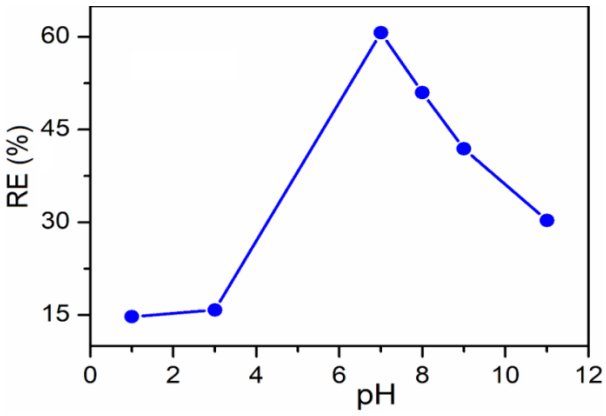

Figure 3. Effect of pH on the adsorption efficiency of OFX on CS-MNPs.

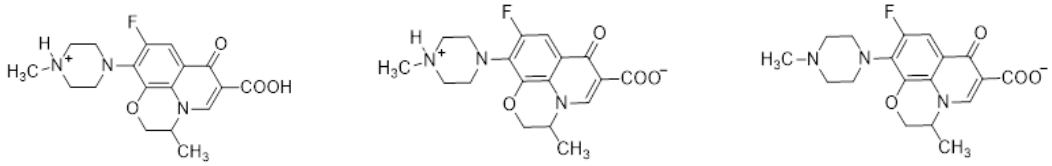

Figure 4. Existing forms of OFX at different pH [20].

3.2.2. Effect of contact time

A period of 5 to 150 min was employed to investigate the influence of contact duration on the effectiveness of OFX adsorption (Figure 5). OFX adsorption efficiency exhibited a sharp increase from 53.55 % to 59.66 % during 5 to 30 min. Subsequently, it increased slowly from 59.66 % to 61.10 % between 30 and 150 min. This observation can be attributed to the fact that after 30 min of adsorption, the adsorption sites on CS-MNPs were nearly saturated with adsorbed OFX, resulting in only marginal improvements in adsorption efficiency with extended contact duration. This suggests that equilibrium in the adsorption process is nearly attained. Consequently, a contact time of 30 min was selected for further research. This trend has also

been reported in some previous studies where the authors investigated the effect of OFX adsorption time on ZnO nanoparticles [20], Oryza sativa husk ash [21], rice husk ash [22], magnetic carbon nanocomposite (MCN) prepared from waste biomass (Dalbergia sissoo sawdust) [23], and GO [24].

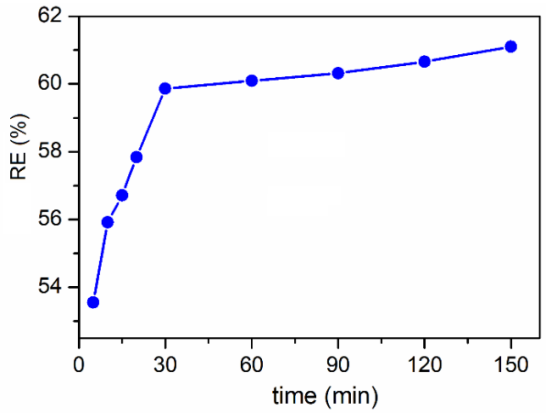

Figure 5. Effect of contact time on OFX removal efficiency.

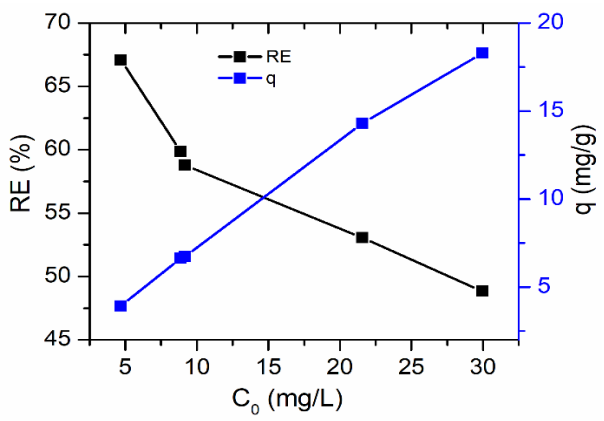

Figure 6. Effect of initial concentration on removal efficiency and adsorption capacity of OFX.

3.2.3. Effect of initial concentration

As the initial concentration of OFX increases from 5 to 30 mg/L within the study's initial concentration range (Figure 6), the adsorption efficiency decreases to 48.85 %, while the adsorption capacity increases from 3.93 mg/g to 18.29 mg/g. This trend can be explained by the fact that as the OFX concentration increases, while the CS-MNP adsorbent mass remains constant, there is a greater competitive adsorption of OFX molecules on the material surface. In other words, when the initial amount of adsorbent remains fixed and the adsorption sites remain constant, the quantity of free OFX in the solution increases, leading to a decrease in adsorption effectiveness. This result aligns with the findings published from previous studies on initial concentrations of the adsorbent [25, 26].

3.2.5. Effect of second antibiotic on OFX adsorption capacity

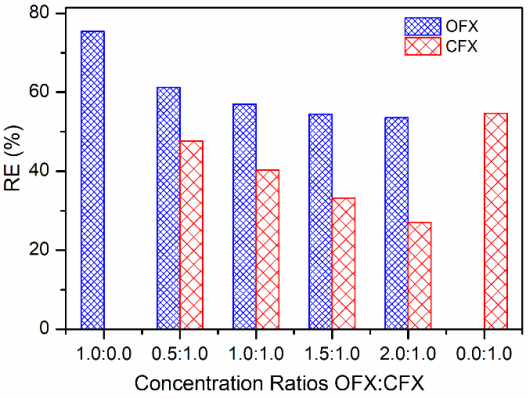

Figure 7. Adsorption efficiency of OFX and CFX from the mixture at different concentration ratios (OFX:CFX).

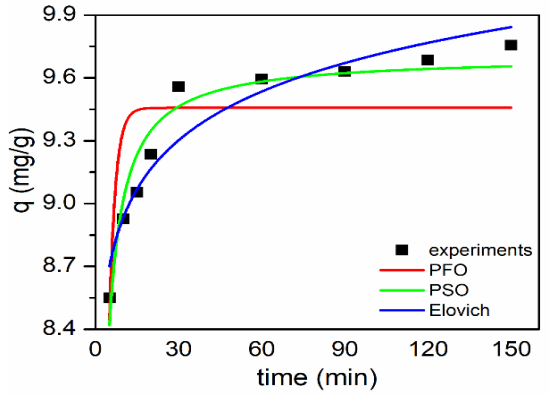

Figure 8. Adsorption kinetic models of OFX onto CS-MNPs.

In fact, wastewater often contains multiple pollutants rather than just a single contaminant [21]. As a broad-spectrum antibacterial antibiotic, ciprofloxacin (CFX) is frequently used. Wastewater often contains substantial quantities of both OFX and CFX, constituting significant surface water contaminants [27].

Therefore, it is crucial to investigate how CFX affects the ability of CS-MNPs to adsorb OFX. Figure 7 illustrates the effectiveness of adsorbing a combination of CFX and OFX in a solution. Across the examined concentration ratios, the presence of CFX in the solution notably affects the efficiency of OFX adsorption. OFX and CFX adsorption efficiencies decreased from 61.51 % to 53.55 % and from 54.67 % to 27.10 %, respectively, as the concentration ratio of OFX:CFX in the solution increased from 0.5:1.0 to 2.0:1.0 (with the OFX concentration varying from 5.01 mg/L to 19.95 mg/L while the CFX concentration remained constant). All these values are lower than the individual adsorption efficiencies of OFX and CFX. This phenomenon may be attributed to the competition between OFX and CFX adsorbates for the adsorption sites on the surface of CS-MNPs, leading to rapid site saturation and reduced efficacy in adsorption for each antibiotic.

3.3. Adsorption models

3.3.1. Adsorption kinetic models

Based on the experimental results obtained on the effect of time, the data were analyzed to determine the adsorption kinetic models. The pseudo-first-order (PFO), pseudo-second-order (PSO), and Elovich equations are given in Equations (3), (4), and (5), respectively [28]:

$$q_t = q_e(1-e^{-K_1 t}) \tag{3}$$

$$q_t = \frac{q_e^2 K_2 t}{1+q_e K_2 t} \tag{4}$$

$$q_t = \frac{1}{\beta}\ln(\alpha\beta) + \frac{1}{\beta}\ln t \tag{5}$$

wherein: q_e (mg/g) and q_t (mg/g) are the adsorption capacities at equilibrium time and time t; K_1 (1/time), and K_2 (g/mg.time) are the reaction rate constants of the pseudo-first-order and pseudo-second-order models, respectively; α (mg/g.min) is the initial speed of the adsorption process; β (g/mg) is the Elovich constant.

Figure 8 shows the results of the models, and Table 1 provides the model's parameter values. Notably, the PFO, PSO, and Elovich kinetic models had correlation coefficient values R^2 of 0.51, 0.95, and 0.91, respectively, with the PSO model exhibiting the highest R^2 value. Furthermore, the maximum adsorption capacity determined by the PSO model (q_e = 9.70 mg/g) closely aligns with the experimental data ($q_{experimental}$ = 9.76 mg/g). These findings demonstrate that the adsorption process of OFX antibiotic follows a second-order kinetic model with a rate constant of K_2 = 0.14 g/mg.min. This result is consistent with previous studies on the adsorption of OFX antibiotics onto various adsorbent materials, including activated carbon [28], metal-organic framework material ZIF-8 [29], and graphene oxide [24].

Based on the results obtained from studying the kinetics of the adsorption process, we can calculate the activation energy of the OFX adsorption onto CS-MNPs using Equation (6) [30]:

$$E_a = RT\,[\ln(K_2 q_e^2) - \ln K_2] \quad (6)$$

where E_a is the activation energy of the adsorption process (J/mol), K_2 is the PSO model's reaction rate constant. At a temperature of 30 ^oC, the OFX adsorption process onto CS-MNPs has an activation energy of 11.45 kJ/mol. This result demonstrates that OFX is physically adsorbed onto CS-MNPs [30].

Table 1. Parameters in adsorption kinetic models.

Model	Parameter	Value
PFO	K_1 (1/min)	0.45
	q_e (mg/g)	9.46
	R^2	0.51
PSO	K_2 (g/mg.min)	0.14
	q_e (mg/g)	9.70
	R^2	0.95
Elovich	α (mg/g.min)	1.2×10^{10}
	β (g/mg)	2.98
	R^2	0.91

3.3.2. Isotherm adsorption models

The experimental data regarding the influence of the initial concentration of OFX were fitted to the Langmuir, Freundlich, and Temkin isotherm adsorption models. The mathematical expressions for the Langmuir, Freundlich, and Temkin models are provided in Equations (7), (8), and (9), respectively [30]:

$$q = q_m \cdot \frac{K_L.C}{1 + K_L.C} \quad (7)$$

$$q = K_F.C^{1/n},\ (n > 1) \quad (8)$$

$$q = \frac{RT}{b_T}\ln(K_T C) \quad (9)$$

wherein: q_m is the maximum capacity (mg/g); K_L is the Langmuir constant ($L.mg^{-1}$). The dimensionless constant R_L is often used to evaluate the suitability of the Langmuir model, which is determined by Equation (10):

$$R_L = \frac{1}{1 + C_0.K_L} \quad (10)$$

if $R_L = 0$, the model is irreversible; if R_L is between 0 – 1, the model is suitable; if $R_L > 1$, the model is not suitable; if $R_L = 1$, the model is linear. K_F is the Freundlich constant, which characterizes the adsorption capacity of the material. n is the Freundlich coefficient. If n is between 1 ÷ 10, it proves that the adsorbent is suitable for the adsorbed substance. K_T (L/mg) is the Temkin constant. b_T (J/mol) is the adsorption energy. R = 8.314 (J/mol.K) is the gas constant. T (K) is the absolute temperature [30].

From Figure 9 and Table 2, it is evident that both the Langmuir and Freundlich models exhibit high correlation values ($R^2 > 0.99$), which are higher than those of the Temkin model ($R^2 = 0.94$). Additionally, the value of the Langmuir constant R_L, determined using Equation (10), falls within the optimal range for the adsorption process (R_L = 0 - 1). The fact that the Freundlich coefficient value R_F falls within the range of 1 to 10 (n = 1.45) indicates that CS-MNPs are an

effective adsorbent for OFX treatment. These findings suggest that both the Langmuir and Freundlich models are suitable for describing the adsorption process of OFX onto CS-MNPs, with a maximum monolayer adsorption capacity of 37.85 mg/g.

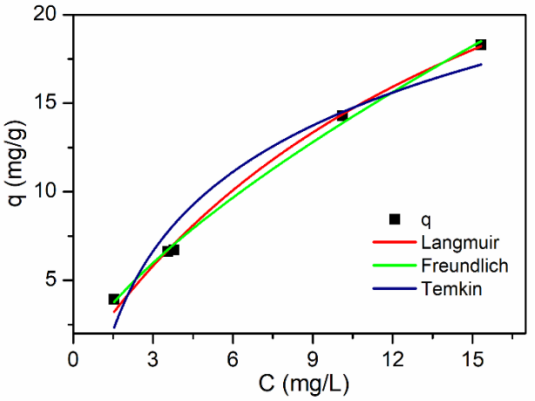

Figure 9. Isotherm adsorption models of OFX onto CS-MNPs.

Table 2. Parameters of the adsorption models.

Langmuir isotherm		Freundlich isotherm		Temkin isotherm	
q_m (mg/g)	37.85	K_F ($mg^{1-(1/n)}.L^{1/n}/g$)	2.80	K_T (L/mg)	0.94
K_L (L/g)	0.06	n	1.45	b_T (J/mol)	383.50
R_L	0.36 - 0.78	R^2	0.997	R^2	0.936
R^2	0.995				

CS-MNPs have a higher maximum adsorption capacity and reach adsorption equilibrium faster than other published materials [21, 22]. Modified bentonite takes 140 hours to reach adsorption equilibrium [31], whereas rice husk ash has a q_m of 6.28 mg/g and a contact time of 430 min [22]. Hence, CS-MNPs can be a valuable substance for future removal of antibiotics from aqueous solutions.

3.3.3. Langmuir competitive adsorption model

The Langmuir competitive adsorption model was developed based on the Langmuir model, which essentially represents monolayer adsorption. This model assumes the presence of multiple adsorbates at the adsorption site. The original form of the Langmuir competitive adsorption equation along with its linear forms are represented by Equations (11), (12) and (13), respectively.

$$q_i = \frac{q_m.K_{Li}.C_i}{1+K_{Li}.C_i+K_{Lj}.C_j} \quad (11)$$

$$\frac{C_i}{C_j.q_i} = \frac{C_i}{q_{mi}.C_j} + \frac{K_j}{K_i.q_{mi}} \quad (12)$$

$$\frac{C_j}{C_i.q_B} = \frac{C_j}{q_{mj}.C_i} + \frac{K_i}{K_j.q_{mj}} \quad (13)$$

wherein: C_i, C_j are the equilibrium concentrations of i, j (mg/L); q_i, q_j are the adsorption capacities of i, j at equilibrium time (mg/g); q_{mi} is the maximum adsorption capacity of substance

i in solution (mg/g); and $K_{Lji} = b_j/b_i$ and $K_{Li} = b_i/b_j$ are parameters representing the heat of adsorption process [20].

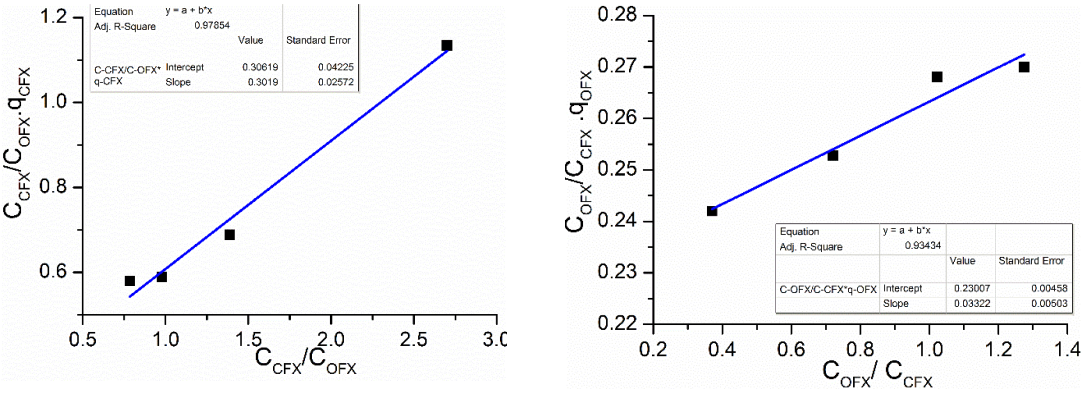

Figure 10. Langmuir competitive adsorption model for ofloxacin - ciprofloxacin system.

Figure 10 illustrates that the simultaneous adsorption of OFX and CFX in solution is well-described by the Langmuir competitive adsorption model with correlation coefficients R^2 of 0.98 and 0.93, respectively. The Langmuir coefficients $K_{L,CFX}$ = 1.01 and $K_{L,OFX}$ = 6.97 are calculated from the model. In solution, CFX and OFX have respective adsorption capacities of 3.31 mg/g and 30.30 mg/g. These values are all lower than those calculated by the Langmuir model ($q_{m,CFX}$ = 53.25 mg/g [32] and $q_{m,OFX}$ = 37.85 mg/g [this study]). These findings demonstrate that the simultaneous adsorption of CFX and OFX is a competitive adsorption process. Due to competition for adsorption sites on the material surface, the adsorption efficiency of a single compound will decrease when another substance is present in the solution at the same time. This result is also consistent with some previously published studies on the adsorption of the Cu(II) - Cd(II) system onto water hyacinth-based adsorbent materials [33], the ciprofloxacin hydrochloride - ofloxacin hydrochloride system and the diclofenac sodium - paracetamol system onto ZnO nanoparticles [20], and the methyl orange - mongo red system onto Mg_2Al-LDH [34].

3.4. Regeneration of adsorption material

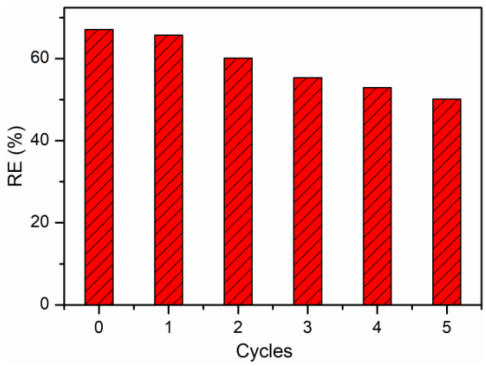

Figure 11. Removal efficiency of ofloxacin from aqueous solution after CS-MNPs reuse cycles.

It can be seen from Figure 11 that the OFX removal efficiency by reused CS-MNPs was lower than that of the initial CS-MNP composites. The OFX removal efficiency decreased from 67.09 % to 50.16 % after five reuses, demonstrating the significant potential of CS-MNPs for

multiple uses. These results indicate that CS-MNPs are highly stable, possess an appropriate adsorption capacity, and exhibit excellent regeneration capability for removing OFX from aqueous solutions.

4. CONCLUSIONS

The in-situ co-precipitation approach was successfully applied in creating CS-MNPs composite materials. The materials have a homogeneous structure with cubic Fe_3O_4 spinel particles of 20 nm size. CS-MNPs exhibit strong magnetic properties and possess the ability to adsorb and remove ofloxacin antibiotic residues from aqueous solutions. The most effective OFX elimination occurs at pH 7 for 30 min. OFX removal efficiency decreases when ciprofloxacin, a second antibiotic, is present in the mixture. The pseudo-second-order adsorption kinetic model, as well as the Langmuir and Freundlich isotherm adsorption models, explain the adsorption of OFX on the CS-MNPs material, indicating physical adsorption. According to the Langmuir model, OFX can be adsorbed up to a maximum of 37.85 mg/g on CS-MNPs. The adsorption of CFX and OFX in solution follows a competitive adsorption pattern, as described by the Langmuir competitive adsorption model. CS-MNPs demonstrate reusability over five cycles, with OFX removal efficiency reaching 50.16 %.

Acknowledgments. The research funding from the Ministry of Education and Training (Grant number: B2023-TNA-27) is acknowledged.

CRediT authorship contribution statement. Bui Minh Quy: Supervision, Investigation, Funding acquisition. Hoang Van Quang: Experiment, Formal analysis. Vu Thi Thu Le: Methodology. Vu Quang Tung: Formal analysis, Investigation. Tran Tuan Tu: Formal analysis, Methodology. Nguyen Thi Quynh Giang: Experiment.

Declaration of competing interest. The authors declare that they have no known competing financial interests or personal relationships that could have appeared to influence the work reported in this paper.

REFERRENCES

1. Kulik K., Lenart-Boroń A., and Wyrzykowska K. - Impact of Antibiotic Pollution on the Bacterial Population within Surface Water with Special Focus on Mountain Rivers, Water **15** (5) (2023) 975. doi: 10.3390/w15050975.
2. Bird K., Boopathy R., Nathaniel R., and LaFleur G. - Water pollution and observation of acquired antibiotic resistance in Bayou Lafourche, a major drinking water source in Southeast Louisiana, USA. Environ. Sci. Pollut. Res. **26** (33) (2019) 34220-34232. doi: 10.1007/s11356-018-4008-5.
3. Binh V. N., *et al.* - Investigation of antibiotics in health care wastewater in Ho Chi Minh City, Vietnam. Sci. Total Environ **692** (7) (2021) 157-174. doi: 10.1007/s10661-016-5704-6.
4. Anh H. Q., *et al.* - Antibiotics in surface water of East and Southeast Asian countries: A focused review on contamination status, pollution sources, potential risks, and future perspectives, Sci. Total Environ. **764** (2021) 142865. doi:10.1016/J.SCITOTENV. 2020.142865.
5. Al-Omar M. A. - Ofloxacin Profiles of Drug Substances, Excipients and Related Methodology Academic Press **34** (2009) 265-298. doi:10.1016/S1871-5125(09)34006-6
6. Salamatinia B. A. P. - A Short Review on Presence of Pharmaceuticals in Water Bodies and the Potential of Chitosan and Chitosan Derivatives for Elimination of Pharmaceuticals, J. Mol. Genet. Med. **S4** (2015) 1-7. doi: 10.4172/1747-0862.S4-001.

7. Karimi-Maleh H., *et al.* - Recent advances in using of chitosan-based adsorbents for removal of pharmaceutical contaminants: A review, J. Clean. Prod. **291** (2021) 125880. doi: 10.1016/j.jclepro.2021.125880.
8. Cao Z., Fan L., Zhang J., Yan P., Wang H., and Dong W. - Degradation of ofloxacin in electro-Fenton system with adsorption and green self-regeneration function, J. Water Process Eng. **48** (2022) 102902. doi: 10.1016/j.jwpe.2022.102902.
9. Dutta J. and Mala A. A. - Removal of antibiotic from the water environment by the adsorption technologies: a review, Water Sci. Technol. **83** (3) (2020) 401-426. doi: 10.2166/wst.2020.335.
10. Panda S. K., *et al*. - Magnetite nanoparticles as sorbents for dye removal: a review, Environ. Chem. Lett. **19** (3) (2021) 2487-2525. doi: 10.1007/s10311-020-01173-9.
11. Shan H., Zeng C., Zhao C., and Zhan H. - Iron oxides decorated graphene oxide/chitosan composite beads for enhanced Cr(VI) removal from aqueous solution, Int. J. Biol. Macromol. **172** (2021) 197-209, doi: 10.1016/j.ijbiomac.2021.01.060.
12. Moradian M., Faraji A. R., and Davood A. - Removal of aflatoxin B1 from contaminated milk and water by nitrogen/carbon-enriched cobalt ferrite -chitosan nanosphere: RSM optimization, kinetic, and thermodynamic perspectives, Int. J. Biol. Macromol. **256** (2024) 127863, doi: 10.1016/j.ijbiomac.2023.127863.
13. Avinash Kadam, Jang J., Lim S. R., and Lee D. S. - Low-Cost Magnetic Fe_3O_4/Chitosan Nanocomposites for Adsorptive Removal of Carcinogenic Diazo Dye, Theor. Found. Chem. Eng. **54** (4) (2020) 655-663. doi: 10.1134/S0040579520040193.
14. Karaca E., *et al*. - Synthesis, characterization and magnetic properties of Fe_3O_4 doped chitosan polymer, J. Magn. Magn. Mater. **373** (2015) 53-59. doi:10.1016/j.jmmm. 2014.02.016.
15. Tandekar S. A., Pande M. A., Shekhawat A., Fosso-Kankeu E., Pandey S., and Jugade R. M. - Fe(III)–Chitosan Microbeads for Adsorptive Removal of Cr(VI) and Phosphate Ions, Minerals **12** (7) (2022) 874. doi: 10.3390/min12070874.
16. Bui Q. M., *et al*. - Removal of Fluoroquinolone Antibiotics by Chitosan–Magnetite from Aqueous: Single and Binary Adsorption, Processes **11 (**8) (2023) 2396. doi:10.3390/ pr11082396.
17. Bui Q. M., Nguyen V. D., Vu T. Q., Nguyen L. T. N., and Nguyen H. T. H. - Removal of anionic dye from aqueous solution by chitosan - magnetite nanocomposite, Int. J. Environ. Anal. Chem. **104** (18) (2024) 6127-6147. doi: 10.1080/03067319.2022.2140410.
18. Erwin A., *et al*. - Magnetic iron oxide particles (Fe_3O_4) fabricated by ball milling for improving the environmental quality, IOP Conf. Ser. Mater. Sci. Eng. **845** (1) (2020) 012051. doi: 10.1088/1757-899X/845/1/012051.
19. Sureshkumar V., Kiruba Daniel S. C. G., Ruckmani K., and Sivakumar M. - Fabrication of chitosan–magnetite nanocomposite strip for chromium removal, Appl. Nanosci. **6** (2) (2016) 277-285. doi: 10.1007/s13204-015-0429-3.
20. Dhiman N. and Sharma N. - Removal of pharmaceutical drugs from binary mixtures by use of ZnO nanoparticles: (Competitive adsorption of drugs), Environ. Technol. Innov. **15** (2019) 100392. doi: 10.1016/j.eti.2019.100392.
21. Dhiman N. - Analysis of non competitive and competitive adsorption behaviour of ciprofloxacin hydrochloride and ofloxacin hydrochloride from aqueous solution using oryza sativa husk ash (single and binary adsorption of antibiotics), Clean. Mater. **5** (2022)

100108. doi: 10.1016/J.CLEMA.2022.100108.

22. Kaur G., Singh N., and Rajor A. - Ofloxacin adsorptive interaction with rice husk ash: Parametric and exhausted adsorbent disposability study, J. Contam. Hydrol. **236** (2021) 103737. doi: 10.1016/j.jconhyd.2020.103737.
23. Wahab M., Zahoor M., and Salman S. M. - A novel approach to remove ofloxacin antibiotic from industrial effluent using magnetic carbon nanocomposite prepared from sawdust of Dalbergia sissoo by batch and membrane hybrid technology, Desalin. WATER Treat. **165** (2019) 83-96. doi: 10.5004/dwt.2019.24573.
24. Yadav S., Goel N., Kumar V., Tikoo K., and Singhal S. - Removal of fluoroquinolone from aqueous solution using graphene oxide: experimental and computational elucidation, Environ. Sci. Pollut. Res. **25** (3) (2018) 2942-2957. doi: 10.1007/s11356-017-0596-8.
25. Yao B., Luo Z., Du S., Yang J., Zhi D., and Zhou Y. - Sustainable biochar/$MgFe_2O_4$ adsorbent for levofloxacin removal: Adsorption performances and mechanisms, Bioresour. Technol. **340** (2021) 125698. doi: 10.1016/j.biortech.2021.125698.
26. Duan W., *et al*. - Enhanced adsorption of three fluoroquinolone antibiotics using polypyrrole functionalized Calotropis gigantea fiber, Colloids Surfaces A Physicochem Eng. Asp. **574** (2019) 178-187. doi: 10.1016/J.COLSURFA.2019.04.068.
27. Szymańska U., Wiergowski M., Sołtyszewski I., Kuzemko J., Wiergowska G., and Woźniak M. K. - Presence of antibiotics in the aquatic environment in Europe and their analytical monitoring: Recent trends and perspectives. Microchem, J. **147** (2019) 729-740. doi: 10.1016/j.microc.2019.04.003.
28. Kong Q., He X., Shu L., and Sheng Miao M. - Ofloxacin adsorption by activated carbon derived from luffa sponge: Kinetic, isotherm, and thermodynamic analyses, Process Saf. Environ. Prot. **112** (2017) 254-264. doi: 10.1016/j.psep.2017.05.011.
29. Yu R. and Wu Z. - High adsorption for ofloxacin and reusability by the use of ZIF-8 for wastewater treatment, Microporous Mesoporous Mater. **308** (2020) 110494. doi:10.1016/ j.micromeso.2020.110494.
30. Munir M., *et al*. - Effective Adsorptive Removal of Methylene Blue from Water by Didodecyldimethylammonium Bromide-Modified Brown Clay, ACS Omega **5** (27) (2020) 16711-16721. doi: 10.1021/acsomega.0c01613.
31. Antonelli R., Martins F. R., Malpass G. R. P., da Silva M. G. C., and Vieira M. G. A. - Ofloxacin adsorption by calcined Verde-lodo bentonite clay: Batch and fixed bed system evaluation, J. Mol. Liq. **315** (2020) 113718. doi: 10.1016/J.MOLLIQ.2020.113718.
32. Vu Quang T., Bui Minh Q., and Hoang Thi D. - Synthesis of chitosan-magnetite composite apply to adsorption antibiotic in aqueous, Vietnam J. Catal. Adsorpt. **10** (1S) (2021) 121-126. doi: 10.51316/jca.2021.104.
33. Nharingo T. and Ngwenya T. J. - Single and binary sorption of lead(II) and zinc(II) ions onto Eichhornia Crassipes (water hyacinth) ash, Int. J. Eng. Sci. Innov. Technol. **2** (4) (2013) 419-426.
34. Abali M., Ichou A. A., and Benhiti R. - Adsorption of Anionic Dyes Using Monoionic and Binary Systems: a Comparative Study, Lett. Appl. NanoBioScience **10** (3) (2021) 2588-2593. doi: 10.33263/lianbs103.25882593.